Electron Transfer Mechanism of Organocobalt Porphyrins. Site of Electron Transfer, Migration of Organic Groups, and Cobalt−Carbon Bond Energies in Different Oxidation States

Shunichi Fukuzumi,*,† Kenichi Miyamoto,† Tomoyoshi Suenobu,† Eric Van Caemelbecke,‡ and Karl M. Kadish*,‡

Contribution from the Department of Applied Chemistry, Faculty of Engineering, Osaka University, Osaka 565-0871, Japan, and Department of Chemistry, University of Houston, Houston, Texas 77204-5641

Received September 16, 1997

Abstract: The chemical or electrochemical oxidations and coupled chemical reactions of (TPP)Co(R) and (TPP)Co(R)(L) where R = Bu, Et, Me, or Ph, L = a substituted pyridine, and TPP = the dianion of tetraphenylporphyrin were investigated in acetonitrile or dichloromethane. The homogeneous one- or two-electron oxidation of the Co(III) σ-bonded complexes was accomplished using $[Fe(phen)_3]^{3+}$ (phen = 1,10-phenanthroline) as an oxidant. The products of the initial oxidation as well as that of the subsequent R group migration from (TPP)Co(R) or (TPP)Co(R)(L) to give the *N*-aryl or *N*-alkyl Co(II) porphyrins were characterized by ESR and UV−vis spectroscopies, while the rates of migration were determined using stopped flow kinetics. The rate constants of R group migration from the metal to nitrogen in $[(TPP)Co(R)]^+$ were found to vary by 6 orders of magnitude upon going from (TPP)Co(Ph) (1.3×10^{-3} s^{-1}) to (TPP)Co(Bu) (1.2×10^{3} s^{-1}) at 298 K in acetonitrile, but no significant differences were observed between $E_{1/2}$ for the first oxidation of (TPP)Co(Ph) or (TPP)Co(Bu). ESR spectra of the transient singly oxidized porphyrins indicate that the six-coordinated derivatives, represented as $[(TPP)Co(R)(MeCN)]^+$ or $[(TPP)Co(R)(L)]^+$ (R = Ph and Me), have a significant d^5 cobalt(IV) character in acetonitrile, while the five-coordinate compounds, $[(TPP)Co(R)]^+$, in dichloromethane can be formulated as Co(III) porphyrin π cation radicals. The formation constants for conversion of (TPP)Co(R) to (TPP)Co(R)(L) were calculated spectroscopically and the logarithmic values vary linearly with the pK_a of the sixth axial ligand. The $E_{1/2}$ values for the first oxidation of (TPP)Co(R)(L) in dichloromethane and the migration rate constants for the R group of $[(TPP)Co(R)(L)]^+$ in acetonitrile are also related to the ligand pK_a. Cobalt−carbon bond dissociation enthalpies and entropies were determined for (TPP)Co(R) and $[(TPP)Co(R)]^+$, and a comparison of these two sets of data reveals that the Co(IV)−carbon bond in the singly oxidized species is significantly weaker than the Co(III)−carbon bond in the neutral complex.

Introduction

The first one-electron oxidation of σ-bonded organocobalt(III) porphyrins is often followed by a metal to nitrogen migration of the σ-bonded organic ligand.[1−4] Singly oxidized σ-bonded cobalt porphyrins have been characterized as containing Co(III) π cation radicals[2,3] rather than Co(IV), and this assignment contrasts with assignments for singly oxidized σ-bonded iron porphyrins[1,5,6] which were proposed to contain Fe(IV) for compounds containing aryl axial ligands. Non-porphyrin complexes containing a cobalt(IV) oxidation state have been obtained upon oxidation of σ-bonded cobalt(III) diglyoximes[7−9] and cobalt(III) complexes of strongly donating macrocyclic ligands,[10] but Co(IV) porphyrins have yet to be reported in the literature.

The first one-electron oxidation of σ-bonded organocobalt(III) porphyrins can involve the metal center, the conjugated π ring system, or the σ-bonded axial ligand with the specific site of electron transfer being related, in large part, to the solution conditions and donor properties of the σ-bonded axial ligand. This is investigated in the present work which utilizes electrochemistry, UV−vis and ESR spectroscopy, and stopped flow

† Osaka University.
‡ University of Houston.

(1) Guilard, R.; Kadish, K. M. *Chem. Rev.* **1988**, *88*, 1121.
(2) Dolphin, D.; Halko, D. J.; Johnson, E. *Inorg. Chem.* **1981**, *20*, 4348.
(3) (a) Callot, H. J.; Cromer, R.; Louati, R. A.; Gross, M. *Nouv. J. Chem.* **1984**, *8*, 765. (b) Callot, H. J.; Metz, F. *J. Chem. Soc., Chem. Commun.* **1982**, 947. (c) Callot, H. J.; Cromer, R. *Tetrahedron Lett.* **1985**, *26*, 3357.
(4) Kadish, K. M.; Han, B. C.; Endo, A. *Inorg. Chem.* **1991**, *30*, 4502.
(5) (a) Ortiz de Montellano, P. R.; Kunze, K. L.; Augusto, O. *J. Am. Chem. Soc.* **1982**, *104*, 3545. (b) Battioni, P.; Mahy, J. P.; Gillet, G.; Mansuy, D. *J. Am. Chem. Soc.* **1983**, *105*, 1399.
(6) (a) Lançon, D.; Cocolios, P.; Guilard, R.; Kadish, K. M. *J. Am. Chem. Soc.* **1984**, *106*, 4472. (b) Balch, A. L.; Renner, M, W. *J. Am. Chem. Soc.* **1986**, *108*, 2603. (c) Guilard, R.; Boisselier-Cocolios, B.; Tabard, A.; Cocolios, P.; Simonet, B.; Kadish, K. M. *Inorg. Chem.* **1985**, *24*, 2509.
(7) Halpern, J.; Topich, J.; Zamaraev, K. I. *Inorg. Chim. Acta* **1976**, *20*, L21.
(8) (a) Halpern, J.; Chan, M. S.; Hanson, J.; Roche, T. S.; Topich, J. A. *J. Am. Chem. Soc.* **1975**, *97*, 1606. (b) Magnuson, R. H.; Halpern, J.; Levitin, I. Ya.; Vol′pin, M. E. *J. Chem. Soc., Chem. Commun.* **1978**, 44. (c) Abley, P.; Dockal, E. R.; Halpern, J. *J. Am. Chem. Soc.* **1972**, *94*, 659. (d) Topich, J.; Halpern, J. *Inorg. Chem.* **1979**, *18*, 1339. (e) Vol′pin, M. E.; Levitin, I. Ya.; Sigan, A. L.: Nikitaev, A. T. *J. Organomet. Chem.* **1985**, *279*, 263.
(9) (a) Anderson, S. N.; Ballard, D. H.; Chrzastowski, J. Z.; Dodd, D.; Johnson, M. D. *J. Chem. Soc., Chem. Commun.* **1972**, 685. (b) Anderson, S. N.; Ballard, D. H.; Johnson, M. D. *J. Chem. Soc., Perkin Trans. II* **1972**, 311. (c) Chopra, M.; Hun, T. S. M.; Leung, W.-H.; Yu, N.-T. *Inorg. Chem.* **1995**, *34*, 5973.
(10) (a) Anson, F. C.; Collins, T. J.; Coots, R. J.; Gipson, S. L.: Richmond, T. G. *J. Am. Chem. Soc.* **1984**, *106*, 5037. (b) Collins, T. J.; Powell, R. D.; Slebodnick, C.; Uffelman, E. S. *J. Am. Chem. Soc.* **1991**, *113*, 8419.

S0002-7863(97)03257-5 CCC: $15.00
Published on Web 03/11/1998

kinetics to investigate the reactivity and spectroscopic properties of singly oxidized organometallic porphyrins of the type $[(TPP)Co(R)]^+$, $[(TPP)Co(MeCN)]^+$, and $[(TPP)Co(R)(L)]^+$ where R = Bu, Et, Me or Ph, MeCN = acetonitrile, L = a substituted pyridine, and TPP = the dianion of tetraphenylporphyrin. The results of this study indicate that a Co(IV) oxidation state may be accessed upon oxidation of (TPP)Co(R) or (TPP)Co(R)(L) under certain experimental conditions, and the high valence state of the cobalt ion in the singly oxidized cobalt porphyrins appears to directly or indirectly influence the rate of migration of the σ-bonded axial ligand. This study also reports the cobalt−carbon bond dissociation enthalpies and entropies of both $(TPP)Co^{III}(R)$ and $[(TPP)Co^{IV}(R)]^+$.

Experimental Section

Materials. Cobalt(II) tetraphenylporphyrin, (TPP)Co, was prepared as described in the literature[11] and then oxidized by oxygen in methanol containing HCl to obtain tetraphenyl porphyrinatocobalt(III) chloride, (TPP)CoCl, which was further purified by recrystallization from methanol. Methylcobalt(III) tetraphenylporphyrin, (TPP)Co(Me), was prepared from a reaction between methylhydrazine and (TPP)CoCl followed by oxidation of the resulting intermediate by oxygen.[12] Reactions involving (TPP)CoCl were performed in chloroform/acetonitrile (5:1 v/v) since the solubility of (TPP)CoCl is larger in this mixed solvent than in neat chloroform or acetonitrile. (TPP)Co(Ph) was prepared according to literature procedures.[13] (TPP)Co(Et) and (TPP)Co(Bu) were prepared from the reaction of (TPP)CoCl with Et_4Sn or Bu_4Sn as described previously.[14] Et_4Sn (4.0×10^{-2} M) was added to a chloroform/acetonitrile (5:1 v/v) solution of (TPP)CoCl (1.0×10^{-2} M), which had been deaerated with argon gas and kept in the dark. The solution was stirred for a few hours, and the (TPP)Co(R) product was recrystallized from methanol.

The purity of (TPP)Co(R) thus obtained was checked by elemental analysis and ^{1}H NMR spectroscopy. Anal. Calcd for $C_{45}H_{31}N_4Co$, (TPP)Co(Me): C, 78.71; H, 4.55; N, 8.16. Found: C, 78.42; H, 4.43; N, 8.14. Anal. Calcd for $C_{46}H_{33}N_4Co$, (TPP)Co(Et): C, 78.85; H, 4.75; N, 8.00. Found: C, 78.67; H, 4.96; N, 7.92. Anal. Calcd for $C_{48}H_{37}N_4Co$, (TPP)Co(Bu): C, 79.11; H, 5.12; N, 7.69. Found: C, 79.03; H, 5.19; N, 7.66. Anal. Calcd for $C_{50}H_{33}N_4Co$, (TPP)Co(Ph): C, 80.20; H, 4.44; N, 7.48. Found: C, 79.95; H, 4.43; N, 7.62. ^{1}H NMR ($CDCl_3/CD_3CN$ 5:1 v/v, 298 K); δ(Me_4Si, ppm) of coordinated alkyl ligand: (TPP)Co(Me), −4.41 (s, 3H); (TPP)Co(Et), −4.93 (t, 3H, J = 7.4 Hz), −3.46 (q, 2H, J = 7.4 Hz); (TPP)Co(Bu), −4.64 (m, 2H, J = 7.7 Hz), −3.54 (t, 2H, J = 7.8 Hz), −1.36 (m, 2H, J = 7.3 Hz), −0.73 (t, 3H, J = 7.3 Hz); (TPP)Co(Ph), 0.37 (d, 2H, J = 8.3 Hz), 4.63 (dd, 2H, J = 8.3, 6.8 Hz), 5.26 (t, 1H, J = 6.8 Hz). Proton resonances of the porphyrin ligand were found at 7.71 (m, 12H), 8.06 (m, 8H), 8.76 (s, 8H). Since the (TPP)Co(R) derivatives are light sensitive,[15] the compounds were kept in the dark.

Tris(1,10-phenanthroline)iron(III) perchlorate, $[Fe(phen)_3](ClO_4)_3$, was prepared by oxidizing the iron(II) complex with ceric sulfate in aqueous H_2SO_4.[16] Acetonitrile and dichloromethane, used as solvents, were purified and dried with CaH_2 according to standard procedures.[17] Spectral grade chloroform was obtained from Wako Pure Chemicals. Pyridine and substituted pyridines (3,5-dichloropyridine, 4-cyanopyridine, 3-chloropyridine, 3-picoline, 3,4-lutidine, and 4-(dimethylamino)-pyridine) were obtained commercially and purified using standard methods.[17] Acetonitrile-d_3 and chloroform-d_3 were obtained from EURISO-TOP, CEA, France. Trifluoroacetic acid was also obtained commercially. Tetrabutylammonium perchlorate (TBAP), obtained from Fluka Fine Chemical, was recrystallized from ethanol and dried in vacuo prior to use.

Product Analysis. One equiv of $[Fe(phen)_3](ClO_4)_3$ (1.0×10^{-2} M) was added to an NMR tube that contained (TPP)Co(R) (1.0×10^{-2} M) in $CD_3CN/CDCl_3$ (1:1 v/v, 0.60 cm^3) under 1.0 atm of argon. The addition of excess CF_3COOH to the solution resulted in demetalation and the porphyrin product was identified as (*N*-RTPP)H on the basis of its ^{1}H NMR spectrum.[12] ^{1}H NMR measurements were performed with a JNM-GSX-400 (400 MHz) NMR spectrometer. ^{1}H NMR (CD_3CN, 298 K); δ(Me_4Si, ppm): (*N*-MeTPP)H, δ −4.08 (s, 3H, *N*-CH_3), 0.07 (s, 1H), 7.9−8.8 (m, 8H), 9.87 (s, 1H); (*N*-EtTPP)H, δ 3.48 (s, 3H), 4.74 (s, 3H), 7.9−8.9 (m, 8H). The yield in each case was determined as 100 ± 10% by comparison of the integrated signal area with those of an internal standard (dioxane).

The Evans NMR method[18a] was used to determine the solution magnetic susceptibility of the paramagnetic Co(II) complex, [(*N*-MeTPP)Co]$^+$. The NMR spectrometer used in this measurement was equipped with a high magnetic field superconducting magnet. Correction has been made to the original Evans equation[18a] according to the literature.[18b] A capillary tube containing the solvent ($CD_3CN/CDCl_3$, 1:1 v/v, 0.2 mL), $[Fe(phen)_3]^{2+}$ (1.0×10^{-2} M), and tetramethylsilane was inserted into an NMR tube which contained (TPP)Co(Me) (1.0×10^{-2} M), $[Fe(phen)_3]^{3+}$ (1.0×10^{-2} M), and tetramethylsilane in $CD_3CN/CDCl_3$ (1:1 v/v, 0.6 mL). A diamagnetic correction for the TPP ligand was made based on the reported value.[19] The change of solvent density with temperature was also taken into account in determination of the solution magnetic susceptibility.[20]

One equiv of $[Fe(phen)_3](ClO_4)_3$ (4.0×10^{-3} M) in deaerated MeCN (0.5 mL) was added with a syringe to a sample tube sealed with a rubber septum that contained (TPP)Co(Me) (4.0×10^{-2} M) in deaerated $CHCl_3$ (0.5 mL). After completion of the reaction, the gaseous products were analyzed by GC using a Unibeads 1-S column. A commercial standard gas from GL Science Co. Ltd, Japan, was used as a reference and contained methane (0.99%), ethane (1.02%), propane (1.01%), isobutane (1.00%), and butane (1.00%). The determination of the yields were made using sample tubes of the same size after equilibrium of the reference gas.

Spectral and Kinetic Measurements. Typically, a 10 μL aliquot of (TPP)Co(R) (1.5×10^{-3} M) in $CHCl_3$ or CH_2Cl_2 was added to a quartz cuvette (10 mm i.d.) which contained $[Fe(phen)_3](ClO_4)_3$ (5.0×10^{-6} M) in deaerated MeCN (3.0 mL). This led to an electron transfer from (TPP)Co(R) to $[Fe(phen)_3](ClO_4)_3$. UV−vis spectral changes associated with this electron transfer were monitored using a Shimadzu UV-2200 spectrophotometer, a Hewlett-Packard 8452A diode array spectrophotometer, or a Hewlett-Packard 8453 diode array spectrophotometer. All experiments were carried out in a dark cell compartment using deaerated solutions. It was confirmed that the thermal rates were not affected by the monitoring light.

Kinetic measurements of the electron transfer from (TPP)Co(R) to $[Fe(phen)_3](ClO_4)_3$ were carried out using a Union RA-103 stopped-flow spectrophotometer. Deaerated MeCN solutions of (TPP)Co(R) and $[Fe(phen)_3](ClO_4)_3$ were transferred to the spectrophotometric cells by means of a glass syringe which had earlier been purged with a stream of argon. All kinetic measurements were carried out under deaerated conditions. The rates of the migration reactions were followed by spectrally monitoring the increase in absorption band intensity due to the oxidized porphyrin product under pseudo-first-order conditions where the concentration of $[Fe(phen)_3]^{3+}$ was maintained at more than 10-fold excess of the (TPP)Co(R) concentration. Pseudo-first-order rate constants were determined by a least-squares curve fit using an NEC microcomputer. The first-order plots of $\ln(A_\infty - A)$ vs time (A_∞ and A are the final absorbance and the absorbance at the reaction time, respectively) were linear for three or more half-lives with the correlation coefficient, $\rho > 0.99$.

(11) Shirazi, A.; Goff, H. M. *Inorg. Chem.* **1982**, *21*, 3420.
(12) Mansuy, D.; Battioni, J.-P.; Duprè, D.; Sartori, E.; Chottard, G. *J. Am. Chem. Soc.* **1982**, *104*, 6159.
(13) Callot, H. J.; Metz, F.; Cromer, R. *Nouv. J. Chem.* **1984**, *8*, 759.
(14) Fukuzumi, S.; Kitano, T. *Inorg. Chem.* **1990**, *29*, 2558.
(15) (a) Kendrick, M. J.; Al-Akhdar, W. *Inorg. Chem.* **1987**, *26*, 3972. (b) Perree-Fauvet, M.; Gaudemer, A.; Boucly, P.; Devynck, J. *J. Organomet. Chem.* **1976**, *120*, 439.
(16) Wong, C. L.; Kochi, J. K. *J. Am. Chem. Soc.* **1979**, *101*, 5593.
(17) Perrin, D. D.; Armarego, W. L. F.; Perrin, D. R. *Purification of Laboratory Chemicals*; Pergamon Press: Elmsford, 1966.
(18) (a) Evans, D. F. *J. Chem. Soc.* **1959**, 2003. (b) Schubert, E. M. *J. Chem. Educ.* **1992**, *69*, 62 and references therein.
(19) Eaton, S. S.; Eaton, G. R. *Inorg. Chem.* **1980**, *19*, 1095.
(20) (a) Hanson, E. S. *Ind. Eng. Chem.* **1949**, *41*, 99. (b) Ostfeld, D.; Cohen, I. A. *J. Chem. Educ.* **1972**, *49*, 829.

The coordination of substituted pyridine as a sixth axial ligand to (TPP)Co(R) in MeCN was monitored by measuring the UV−vis spectral changes as a function of the ligand concentration.

ESR Measurements. The ESR spectra of chemically generated $[(TPP)Co(R)]^+$, $[(TPP)Co(R)(MeCN)]^+$, and $[(TPP)Co(R)(L)]^+$ were measured at both room temperature, 203 K, and 77 K (in frozen solutions) with a JEOL X-band spectrometer (JES-ME-LX or JES−RE1XE). Typically a $CHCl_3$ solution of 10 mM (TPP)Co(R) was deaerated in an ESR tube with argon bubbling, and after which it was placed in the cavity that was thermostated with a JEOLDVD Unit (ES-DVT3). The *g* values were calibrated with a Mn^{2+} marker, and the hyperfine coupling constants were determined by computer simulation using a Calleo ESR[a] II program coded by Calleo Scientific Software Publishers. The areas of ESR signals are compared between $[(TPP)Co(Me)(MeCN)]^+$ and $[(TPP)Co]^{2+}$ by correcting the difference in the *g* values.

Cyclic Voltammetry. Redox potentials of (TPP)Co(R) in MeCN or CH_2Cl_2 containing 0.10 M TBAP as supporting electrolyte were determined at room temperature or 203 K by cyclic voltammetry under deaerated conditions in the dark using a three electrode system and a BAS 100B electrochemical analyzer. The working and counter electrodes were platinum, while $Ag/AgNO_3$ (0.01M) was used as the reference electrode. All potentials are reported as V vs SCE. The $E_{1/2}$ value of ferrocene used as a standard is 0.37 V vs SCE in MeCN under our solution conditions.

Results and Discussion

Electron Transfer Oxidation of (TPP)Co(R) by $[Fe(phen)_3]^{3+}$. The electron transfer from (TPP)Co(R) (R = Me, Et, Bu, or Ph) to $[Fe(phen)_3]^{3+}$ is rapid in MeCN at 298 K as indicated by the almost instantaneous formation of $[Fe(phen)_3]^{2+}$ (λ_{max} = 508 nm). When 1 equiv of $[Fe(phen)_3]^{3+}$ is added to an MeCN solution of (TPP)Co(Ph), the Soret band of (TPP)Co(Ph) at 408 nm disappears as $[(TPP)Co(Ph)]^+$ (λ_{max} = 434, 410, 380 nm) is generated. This rapid reaction is then followed by a slow migration of the phenyl group from cobalt to one of the four nitrogens of the macrocycle to yield $[(N\text{-PhTPP})Co]^+$ (λ_{max} = 436 nm) as a final porphyrin product. The UV−visible spectrum of $[(TPP)Co(Ph)]^+$ (λ_{max} = 434, 410 nm) is similar to the UV−visible spectrum of $[(TPP)Co]^{2+}$ (λ_{max} = 433, 414 nm) which is generated by the two-electron oxidation of (TPP)Co with $[Fe(phen)_3]^{3+}$. Since $[(TPP)Co]^{2+}$ is known to be a π radical cation,[21,22] the similar absorption spectra of $[(TPP)Co(Ph)]^+$ and $[(TPP)Co]^{2+}$ show a significant contribution of TPP π radical cation in $[(TPP)Co(Ph)]^+$. In the case of $[(TPP)Co(Me)]^+$ and $[(TPP)Co(Et)]^+$, however, the 406 nm absorption band of the singly oxidized product is significantly stronger than the shoulder band at 410 nm for $[(TPP)Co(Ph)]^+$ (see Figure 1, where the spectrum of $[(TPP)Co(Et)]^+$ was measured at 233 K to slow the migration). Such a difference in the absorption spectra suggests that the abstraction of an electron from [(TPP)Co(R)] (R = Me and Et) may involve the metal rather than the conjugated porphyrin ligand to yield the Co(IV) oxidation state.

The final migration product is the doubly oxidized, $[(N\text{-RTPP})Co]^{2+}$, when 2 equiv of $[Fe(phen)_3]^{3+}$ are reacted with (TPP)Co(R). The final porphyrin product obtained after demetalation was identified as (*N*-RTPP)H by its ^1H NMR spectrum (see Experimental Section). Methane, formed via homolytic cleavage of the Co−Me bond in $[(TPP)Co(Me)]^+$, was also detected as a minor product (5% yield) in the one-electron oxidation of (TPP)Co(Me) (see Experimental Section).

Kinetics of Migration. Migration rates of the σ-bonded ligand of $[(TPP)Co(R)]^+$ (R = Ph and Me) were followed by monitoring the product absorption band as $[(N\text{-RTPP})Co]^+$ is produced after addition of 1 equiv of $[Fe(phen)_3]^{3+}$ to (TPP)Co(R) in MeCN at 298 K. The migration rates of $[(TPP)Co(Me)]^+$ were also obtained by monitoring the change in absorption as $[(N\text{-MeTPP})Co^{III}]^{2+}$ is produced by a two-electron oxidation of (TPP)Co(Me) using more than 2 equiv of $[Fe(phen)_3]^{3+}$ in MeCN at 298 K. The rates for the two-electron oxidation of (TPP)Co(Me) obey first-order kinetics.

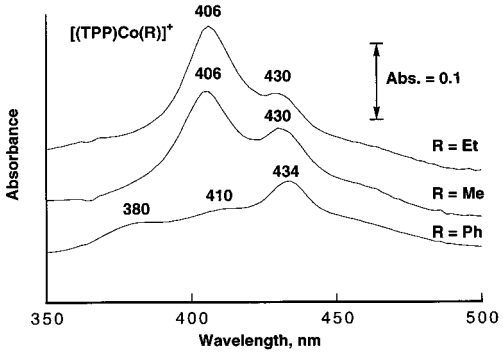

Figure 1. Visible absorption spectra of $[(TPP)Co(R)]^+$ (R = Et, Me, and Ph) observed upon mixing (TPP)Co(R) (5.0×10^{-6} M) and $[Fe(phen)_3](ClO_4)_3$ (5.0×10^{-6} M) at 233 K for (TPP)Co(Et) and at 298 K for (TPP)Co(R) (R = Me and Ph) in MeCN. All measurements were made 1 s after mixing.

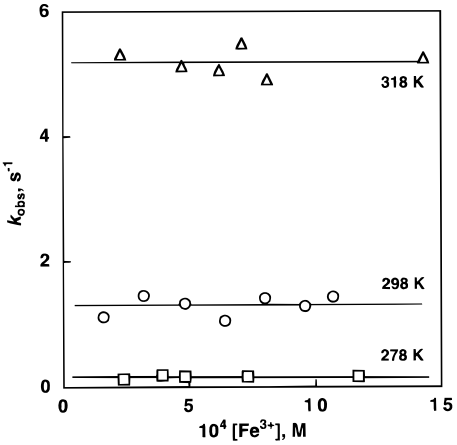

Figure 2. Plot of k_{obs} vs $[Fe^{3+}]$ for electron transfer from (TPP)Co(Me) (5.0×10^{-6} M) to $[Fe(phen)_3]^{3+}$ in deaerated MeCN at different temperatures.

The dependence of the observed first-order rate constant (k_{obs}) on the $[Fe(phen)_3]^{3+}$ concentration was determined at different temperatures, and a summary of the data (Figure 2) shows that the k_{obs} value is independent of changes in the $[Fe(phen)_3]^{3+}$ concentration, which is represented as $[Fe^{3+}]$. This result suggests that the Me group migration is the rate-determining step in the two-electron oxidation of (TPP)Co(Me).

The R group migration of (TPP)Co(Et) and (TPP)Co(Bu) is too fast to be followed by conventional UV−visible spectroscopy, and stopped-flow methods were therefore utilized to follow the migration. The rate of $[(N\text{-RTPP})Co]^{2+}$ formation during the two-electron oxidation of [(TPP)Co(R)] (R = Et or Bu) with a large excess $[Fe(phen)_3]^{3+}$ also obeys first-order kinetics in MeCN at 298 K. The dependence of the observed first-order rate constant (k_{obs}) on the $[Fe(phen)_3]^{3+}$ concentration at different temperatures is shown in Figure 3 for R = Et. A similar result was obtained for R = Bu. In each case the k_{obs} value increases with increase in the $[Fe(phen)_3]^{3+}$ concentration to approach a constant value which corresponds to the migration rate constant (k_{mig}). Such a dependence of k_{obs} on the [Fe-

(21) (a) Ohya-Nishiguchi, H.; Khono, M.; Yamamoto, K. *Bull. Chem. Soc. Jpn.* **1981**, *54*, 1923. (b) Ichimori, K.; Ohya-Nishiguchi, H.; Hirota, N.; Yamamoto, K. *Bull. Chem. Soc. Jpn.* **1985**, *58*, 623.

(22) Dolphin, D.; Felton, R. H. *Acc. Chem. Res.* **1974**, *7*, 26.

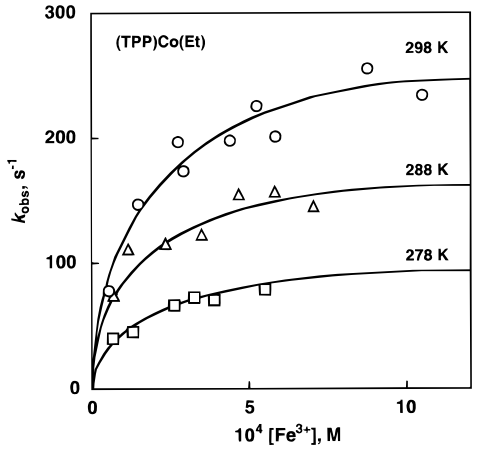

Figure 3. Plot of k_{obs} vs [Fe^{3+}] for electron transfer from (TPP)Co(Et) (5.0×10^{-5} M) to [Fe(phen)$_3$]$^{3+}$ in deaerated MeCN at different temperatures.

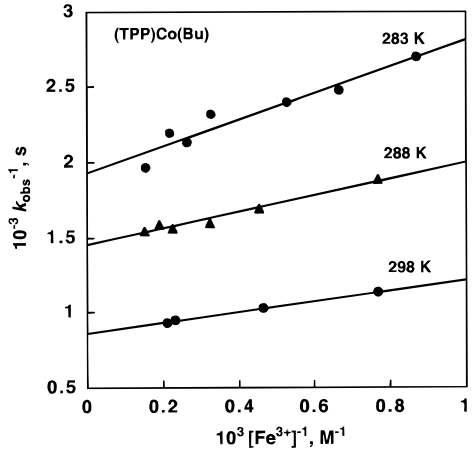

Figure 4. Plot of k_{obs}^{-1} vs [Fe^{3+}]$^{-1}$ for electron transfer from (TPP)Co(Bu) (5.0×10^{-5} M) to [Fe(phen)$_3$]$^{3+}$ in deaerated MeCN at different temperatures.

Scheme 1

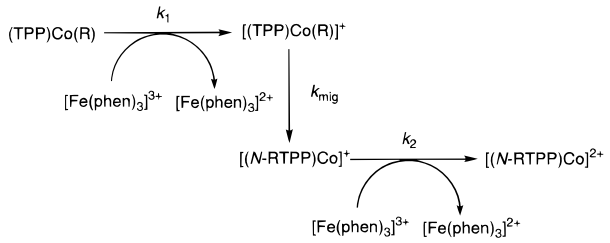

(phen)$_3$]$^{3+}$ concentration can be explained by the sequence of steps shown in Scheme 1, where k_1, k_{mig}, and k_2 represent rate constants of the initial electron transfer from (TPP)Co(R) to [Fe(phen)$_3$]$^{3+}$, the R group migration from [(TPP)Co(R)]$^+$ to [(*N*-RTPP)Co]$^+$, and the following electron transfer from [(*N*-RTPP)Co]$^+$ to [Fe(phen)$_3$]$^{3+}$, respectively.

By applying the steady-state approximation to the intermediates in Scheme 1, the dependence of k_{obs} on the concentration of [Fe(phen)$_3$]$^{3+}$ can be derived as shown in eq 1, where [Fe(phen)$_3$]$^{3+}$ is represented as Fe^{3+} (for the derivation, see Supporting Information). When the initial electron transfer in Scheme 1 is the rate-determining step, i.e., $k_1 \ll k_{mig}$ and k_2, eq 1 is reduced to $k_{obs} \cong k_1[Fe^{3+}]$. On the other hand, when the migration is the rate-determining step, i.e., $k_{mig} \ll k_1$ and k_2, eq 2 is reduced to $k_{obs} \cong k_{mig}$. Equation 1 can be rewritten in the form of eq 2 which predicts a linear correlation between k_{obs}^{-1} and [Fe^{3+}]$^{-1}$.

$$k_{obs} = k_1 k_{mig} k_2[Fe^{3+}]/\{k_{mig}(k_1 + k_2) + k_1 k_2[Fe^{3+}]\} \quad (1)$$

$$k_{obs}^{-1} = \{k_1 k_2[Fe^{3+}]/(k_1 + k_2)\}^{-1} + k_{mig}^{-1} \quad (2)$$

Although the steady-state approximation to derive eq 2 may not be exactly valid when $k_{mig} \approx k_1$, eq 2 can be used to extrapolate the k_{mig} value as shown by the linear plot of k_{obs}^{-1} vs [Fe^{3+}]$^{-1}$ in Figure 4 for R = Bu. A linear plot of k_{obs}^{-1} vs [Fe^{3+}]$^{-1}$ for R = Et was also obtained for the data in Figure 3. The k_{mig} values at different temperatures obtained from the intercepts of the linear plots are listed in Table 1.

The migration rate constants vary by 6 orders of magnitude between the different [(TPP)Co(R)]$^+$ complexes and increase with increase in the electron donor ability of R from R = Ph (1.3×10^{-3} s^{-1}) to R = Bu (1.2×10^3 s^{-1}) in MeCN at 298 K.[23]

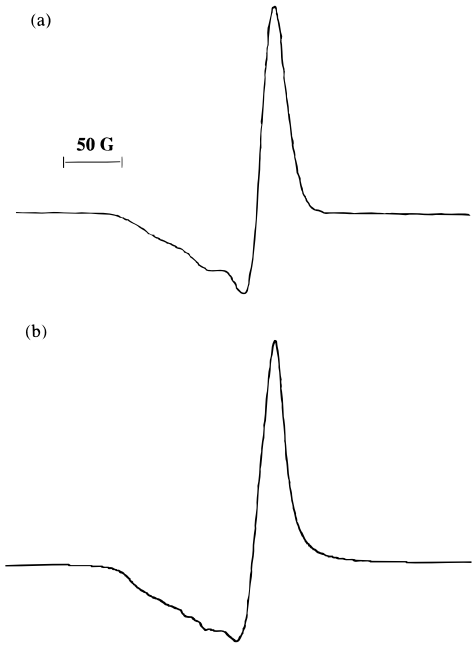

Figure 5. (a) Experimental ESR spectrum and (b) computer simulation spectrum of [(TPP)Co(Me)]$^+$ (1.0×10^{-3} M) generated by addition of [Fe(phen)$_3$]$^{3+}$ (1.0×10^{-3} M) to (TPP)Co(Me) in MeCN/$CHCl_3$ (v:v 1/1) at 77 K.

ESR Spectra of Oxidized Complexes of (TPP)Co(R). The Me group migration rate constant of [(TPP)Co(Me)]$^+$ in MeCN ranges from 1.7×10^{-3} s^{-1} at 278 K to 5.2×10^{-2} s^{-1} at 318 K (see Table 1), and the rate is slow enough at 298 K so that the ESR spectrum of [(TPP)Co(Me)]$^+$ could be measured at 77 K just after the one-electron-transfer oxidation of (TPP)Co(Me) (2.0×10^{-3} M) by Fe(phen)$_3^{3+}$ (2.0×10^{-3} M) in MeCN/$CHCl_3$ (1:1 v/v). This spectrum is shown in Figure 5a. The spectrum exhibits an anisotropic signal with a broad line which reflects coupling of the unpaired electron with the nuclear spin of ^{59}Co ($I = 7/2$), but the hyperfine structure is not well resolved. The computer simulation spectrum is shown in Figure 5b and gives the ESR parameters $g_1 = 2.067$, $g_2 = 2.009$, $g_3 = 2.005$, $A_{1Co} = 11.6$ G, $A_{2Co} = 3.8$ G, $A_{3Co} = 3.0$ G.

The ESR spectrum of [(TPP)Co(Me)]$^+$ could also be measured in solution at 298 K and gives isotropic g (2.027 ± 0.001)

(23) Despite the large variation in the k_{mig} values, they were determined as those independent of [Fe^{3+}] when the migration is always the rate-determining step.

Table 1. Rate Constants for Migration of R Group of $[(TPP)Co(R)]^+$ in MeCN at Various Temperatures

	k_{mig}, s^{-1} [a]						
R	278 K	283 K	288 K	298 K	303 K	318 K	323 K
Bu	*b*	5.2×10^2	6.9×10^2	1.2×10^3	*c*	*c*	*c*
Et	8.5×10^1	*b*	1.7×10^2	2.6×10^2	*b*	*b*	*b*
Me	1.7×10^{-3}	*b*	*b*	1.4×10^{-2}	*b*	5.2×10^{-2}	*b*
Ph	*b*	*b*	*b*	1.3×10^{-3}	2.0×10^{-3}	7.1×10^{-3}	1.0×10^{-2}

[a] The experimentl error is ±5%. [b] Not measured. [c] Too fast to be determined accurately.

Table 2. Isotropic g and A_{Co} Values of $[(TPP)Co(R)]^+$ at 298 K or 203 K in a Mixed $MeCN/CHCl_3$ or $EtCN/CHCl_3$ Solvent (1:1 v/v)

	g (A_{Co}, G)	
R	$MeCN/CHCl_3$	$EtCN/CHCl_3$
Bu		2.034 (19.0)[a]
Et		2.033 (15.2)[a]
Me	2.027 (7.0)	2.026 (7.0)
Ph	2.015 (5.3)	2.015 (6.2)

[a] Measured in liquid solutions at 203 K.

and A_{Co} (7.0 G) values which agree within experimental error with the values obtained as the average of the anisotropic g values (2.027 ± 0.002) and A_{Co} values (6.1 ± 1.0 G). The ESR spectra of $[(TPP)Co(Et)]^+$ and $[(TPP)Co(Bu)]^+$ could also be measured in propionitrile (EtCN) and $CHCl_3$ (1:1 v/v) at 203 K, and the g and A_{Co} values under these experimental conditions are listed in Table 2. Propionitrile was used in place of acetonitrile in order to avoid freezing of the solvent. In neither case, additional ligand superhyperfine structure attributed to interaction of the unpaired electron with the nitrogen nuclei of the porphyrin ligand could be observed.

A comparison of the g and A_{Co} values of $[(TPP)Co(R)]^+$ (R = Me, Et, Bu) to those of the $[(TPP)Co^{III}]^{2+}$ porphyrin π radical cation ($g = 2.003$, $A_{Co} = 6.0$ G)[21] and several non-porphyrin Co(IV) complexes ($g = 2.020-2.033$, $A_{Co} = 12.3-15.5$ G)[7] suggests that $[(TPP)Co(R)]^+$ can best be described as a d^5 cobalt(IV) complex rather than as a cobalt(III) π radical cation. The absence of superhyperfine splitting due to nitrogen nuclei of the porphyrin ligand suggests that the unpaired electron is predominantly localized in the π-type d_{xy} rather than the σ-type $d_{x^2-y^2}$ orbital. In contrast, an appreciable hyperfine due to nitrogen nuclei ($A_N = 2.8$ G) is observed in the $(TPP)CoCl_2$ π radical cation, and there is a linear correlation between A_{Co} and A_N when the counter anions are changed.[21] In this case, the Co superhyperfine is induced by spin polarization of the σ-electron spin density in the Co−N bonds.[21] In the case of a tetrahedral tetrakis(1-norbonyl)cobalt(IV) complex,[24] however, the unpaired electron may be localized in a σ-type orbital, and the ESR spectrum shows a large anisotropy ($g_\perp = 1.984$, $g_\parallel = 2.036$) with large Co hyperfine splitting ($|A_\perp| = 120$ G, $|A_\parallel| = 40$ G).[25]

The ESR spectrum of $[(TPP)Co(Ph)]^+$ exhibits hyperfine structure due to ^{59}Co, both at 77 and 203 K, and the determined g and A_{Co} values are listed in Table 2. The g (2.015 ± 0.001) and A_{Co} (6.2 ± 0.5 G) values of $[(TPP)Co(Ph)]^+$ are significantly smaller than those of the other $[(TPP)Co(R)]^+$ derivatives (R = Me, Et, and Bu). This indicates a significant contribution of the limiting formal representation in $[(TPP)Co(Ph)]^+$ as a d^6 cobalt(III) porphyrin π cation radical as opposed to the other $[(TPP)Co(R)]^+$ derivatives (R = Me, Et, and Bu) which have a large amount of Co(IV) character.[26]

The effective magnetic moment, μ_{eff}, of $[(N\text{-MeTPP})Co]^+$ in $CD_3CN/CDCl_3$ (1:1 v/v) is 4.4 μ_B at 298 K based on solution magnetic susceptibility measurements using the Evans NMR method (see Experimental Section). This magnetic moment indicates an $S = 3/2$ spin state which is consistent with a high spin d^7 Co(II) complex.[27] An ESR signal could not be detected for $[(N\text{-MeTPP})Co^{II}]^+$ at the liquid He temperature, and this is probably due to the fast relaxation time of Co(II).[28]

The oxidation of $[(N\text{-MeTPP})Co^{II}]^+$ with excess $Fe(phen)_3^{3+}$ leads to a diamagnetic Co(III) complex. The ESR spectrum of the product obtained after the migration and subsequent electron transfer when (TPP)Co(Me) (1.0×10^{-3} M) is mixed with 2 equiv of $Fe(phen)_3^{3+}$ (2.0×10^{-3} M) in $CH_3CN/CHCl_3$ (1:1 v/v) shows a signal at $g = 2.004$ with $A_{Co} = 9.0$ G, which is assigned to $[(TPP)Co]^{2+}$. However, a comparison of the ESR signal intensity obtained by double integration of the first derivative signal for $[(TPP)Co(Me)]^+$ and $[(TPP)Co]^{2+}$ indicates that only 5 ± 1% of the initial (TPP)Co(Me) complex is converted to $[(TPP)Co]^{2+}$. This agrees with the fact that methane was detected as a minor product (5 ± 0.5% yield) via homolytic cleavage of the Co−Me bond in $[(TPP)Co(Me)]^+$ (*vide supra*). Thus, the overall stoichiometry of the reaction is given by eq 3, where the hydrogen source of methane is not included.

$$(TPP)Co(Me) + 2[Fe(phen)_3]^{3+} \rightarrow 0.95[(N\text{-MeTPP})Co]^{2+} + 0.05[(TPP)Co]^{2+} + 0.05CH_4 + 2[Fe(phen)_3]^{2+} \quad (3)$$

This part of the mechanism is shown in Scheme 2 for the case of (TPP)Co(Me).

The ESR spectra indicate that the initial electron-transfer oxidation of (TPP)Co(Me) leads to $[(TPP)Co(Me)]^+$ which has a significant d^5 cobalt(IV) character rather than to a Co(III) porphyrin π radical cation. The formation of methane as one of the oxidation products indicates that a homolytic cleavage of the Co−Me bond of $[(TPP)Co(Me)]^+$ occurs to give methyl radicals, a minor part of which leads to the formation of methane by hydrogen abstraction from the solvent.[29] However, a major part of the methyl radicals is "trapped" by a nitrogen of the porphyrin ring to yield the final migrated product, $[(N\text{-MeTPP})Co]^+$. A radical addition to the nitrogen of the porphyrin ring

(24) (a) Byrne, E. K.; Theopold, K. H. *J. Am. Chem. Soc.* **1989**, *111*, 3887. (b) Byrne, E. K.; Theopold, K. H. *J. Am. Chem. Soc.* **1987**, *109*, 1282. (c) Bower, B. K.; Tennent, H. G. *J. Am. Chem. Soc.* **1972**, *94*, 2512.

(25) Bower, B. K.; Findlay, M.; Chien, J. C. W. *Inorg. Chem.* **1974**, *13*, 759.

(26) A similar conclusion was made for a phenyl σ-bonded cobalt corrole, (OEC)Co(Ph), where OEC is the trianion of 2,3,7,8-12,13,17,18-octaethylcorrole; (OEC)Co(Ph) can best be represented as a resonance hybrid between a cobalt(III) π radical cation and a cobalt(IV) corrole, see: Will, S.; Lex, J.; Vogel, E.; Adamian, V. A.; Van Caemelbecke, E.; Kadish, K. M. *Inorg. Chem.* **1996**, *35*, 5577.

(27) The spin value for the d^7 spin sate ($S = 3/2$) of a high spin $CoCl_4^{2-}$ is 4.59 μ_B, see: Cotton, A. F.; Wilkinson, G. *Advanced Inorganic Chemistry*; John Wiley & Sons: New York, 1980; p 772.

(28) The ESR spectra of low spin cobalt(II) complexes have been well-characterized in frozen media but cannot be detected in solution because of their short spin−lattice relaxation time, see: Walker, F. A. *J. Am. Chem. Soc.* **1970**, *92*, 4235. Wayland, B. B.; Minkiewicz, J. V.; Abd-Elmageed, M. E. *J. Am. Chem. Soc.* **1974**, *96*, 2795. Wayland, B. B.; Abd-Elmageed, M. E. *J. Am. Chem. Soc.* **1974**, *96*, 4809.

Scheme 2

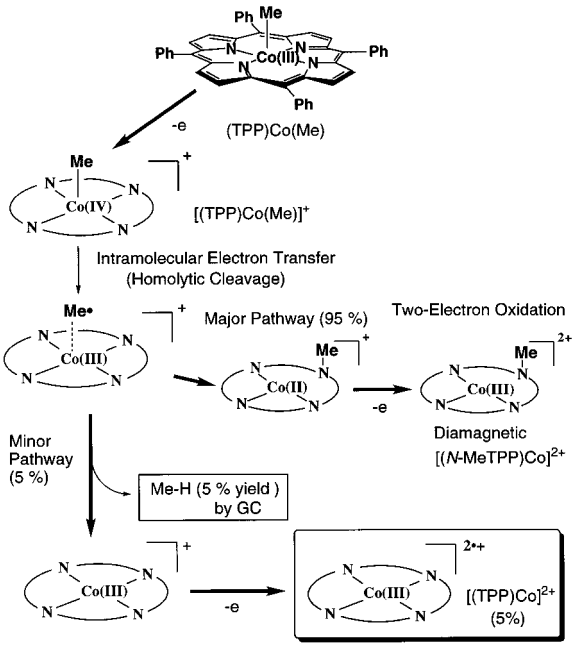

results in cleavage of one nitrogen−cobalt bond, accompanied by a reduction of Co(III) to give $[(N\text{-MeTPP})Co^{II}]^+$ as a major porphyrin product (Scheme 2).

The R group migration rate increases with increase in the electron donor ability of R (in the order Ph < Me < Et < Bu, see Table 1), and this trend suggests that an intramolecular electron transfer from the R group to the Co(IV) metal of $[(TPP)Co(R)]^+$ is the rate-determining step in the homolytic cleavage of the $Co^{IV}-R$ bond. In such a case, the higher oxidation state of the cobalt center will facilitate an intramolecular electron transfer from the R group to the metal center. Thus, the stronger the donor ability of R, the more the d^5 cobalt(IV) character in $[(TPP)Co(R)]^+$ and the faster will be the migration rate, as is experimentally observed in this study. Further support for the mechanism shown in Scheme 2 is given on the following pages.

Cyclic Voltammetry. Slow scan cyclic voltammograms of (TPP)Co(R) (R = Ph and Me) in MeCN/$CHCl_3$ exhibit two reversible oxidations as shown in Figure 6a. Both processes are reversible at room temperature, and this is expected due to the slow migration rates of $[(TPP)Co(Ph)]^+$ and $[(TPP)Co(Me)]^+$ (see Table 1). In contrast, the cyclic voltammograms of (TPP)Co(Et) and (TPP)Co(Bu) at 298 K show a well defined anodic peak for the first oxidation but no coupled cathodic peak. This is consistent with the facile migration of the alkyl group in the singly oxidized species and is shown in Figure 6b for the case of (TPP)Co(Et) at 298 K. The voltammograms of the Et and Bu derivatives become reversible at 203 K as shown for (TPP)Co(Et) in Figure 6b, since the migration rates are significantly slower at this temperature. The one-electron oxidation potentials of (TPP)Co(R) in CH_2Cl_2 or MeCN/$CHCl_3$ at 298 and 203 K are listed in Table 3.

The first oxidation potential of (TPP)Co(R) is reversible in CH_2Cl_2 at 203 K and changes only slightly with decrease in

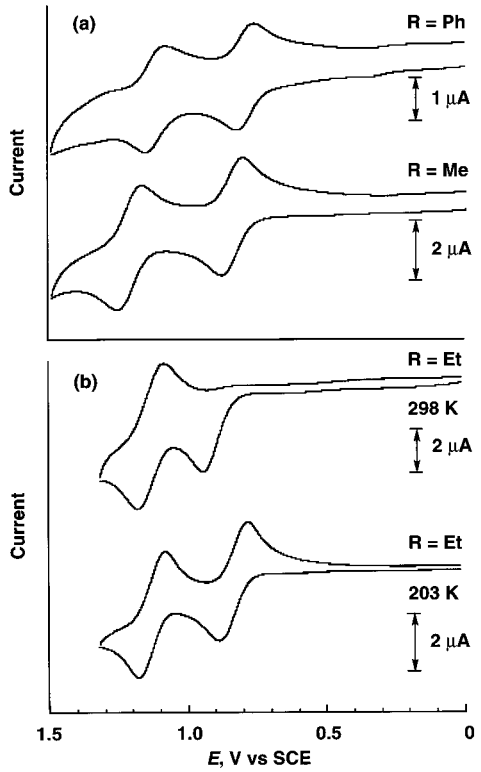

Figure 6. Cyclic voltammograms measured at a scan rate of 0.10 V s^{-1} for 1.0 mM (TPP)Co(R) where (a) R = Ph or Me, T = 298 K and the solvent is MeCN/$CHCl_3$ and (b) R = Et, T = 298 or 203 K and the solvent is CH_2Cl_2.

Table 3. Oxidation Potentials (V vs SCE) of (TPP)Co(R) in CH_2Cl_2 and MeCN/$CHCl_3$ Mixed Solvent Containing 0.1 M TBAP at 298 and 203 K

	$E_{1/2}$, V vs SCE	
R	298 K	203 K
n-Bu	0.96[a] (0.84[a,b])	0.81
Et	0.95[a] (0.83[a,b])	0.84
Me	0.95 (0.84[c])	0.85
Ph	0.98 (0.79[b])	0.89

[a] Anodic peak potential, E_{pa} at 0.1 V s^{-1}. [b] Measured in MeCN/$CHCl_3$ (4:1 v/v). [c] Measured in MeCN/$CHCl_3$ (1:4 v/v).

electron donor ability of the σ-bonded ligand upon going from R = Bu to R = Ph (Table 3). This lack of a dependence on the (TPP)Co(R) oxidation potential by the σ-bonded ligand is consistent with an assignment of the HOMO orbital of (TPP)Co(R) as a π-type d_{xy} orbital which is orthogonal to the axial σ-orbital (*vide supra*). The oxidation potentials of (TPP)Co(R) in CH_2Cl_2 at 298 K are significantly more positive than the potentials in MeCN/$CHCl_3$ (shown in parentheses in Table 3). Such a difference in potentials between the two solvents indicates that MeCN acts as a sixth axial ligand to give $[(TPP)Co(R)(MeCN)]^+$ and the electron donation of the ligand results in a negative shift of the oxidation potential for (TPP)Co(R) in MeCN/$CHCl_3$ as compared to the five-coordinate compound in CH_2Cl_2. In this case, the sixth axial ligand may act as a π-donor.

Effects of Base on Oxidation Potentials of (TPP)Co(R). The addition of pyridine to an MeCN solution of (TPP)Co(Et) results in a significant change in the UV−vis spectrum. From these changes, the formation constants for axial ligand binding of the six substituted pyridines to (TPP)Co(R) were determined in MeCN depending on the pK_a values of the substituted pyridines which vary from 0.67 for 3,5-Cl_2Py to 9.71 for

(29) The formation of methane as a minor product in the electron-transfer oxidation of (TPP)Co(Me) is reminiscent of minor radical products produced in dealkylation of alkylcobalt(III) complexes with iodine, which occurs via electron transfer from alkylcobalt(III) complexes to iodine, followed by the facile homolytic cleavage for the cobalt−carbon bond of the alkylcobalt(IV) complexes, see: Ishikawa, K.; Fukuzumi, S.; Tanaka, T. *Inorg. Chem.* **1989**, *28*, 1661.

Table 4. Halfwave Potentials (V vs SCE) for the Oxidation of (TPP)Co(R)(L) at 298 K in CH_2Cl_2 or MeCN/$CHCl_3$ Containing 1.0 × 10^{-2} M Substituted Pyridine (L) and 0.1 M TBAP

sixth axial ligand, L			σ-bonded ligand, R		
no.	type	pK_a	Et	Me	Ph
	none		0.84[a]	0.95 (0.84[b])	0.98 (0.79[c])
1	3,5-Cl_2Py	0.67	0.77[a]	0.91	0.91 (0.79[c])
2	4-CNPy	1.86	0.74[a]	0.88	0.89 (0.78[c])
3	3-ClPy	2.81	0.72[a]	0.84	0.86 (0.75[c])
4	Py	5.28	0.68[a]	0.76	0.78 (0.75[c])
5	3-MePy	5.79	0.69[a]	0.76	0.78 (0.75[c])
6	3,4-Me_2Py	6.46	0.65[a]	0.73	0.76 (0.73[c])
7	4-NMe_2Py	9.71	0.63[a]	0.66	0.72 (0.69[c])

[a] At 203 K. [b] Measured in MeCN/$CHCl_3$ (1:4 v/v). [c] Measured in MeCN/$CHCl_3$ (4:1 v/v).

4-NMe_2Py.[30] A summary of the values of formation constants is given in Supporting Information. The $E_{1/2}$ values for oxidation of (TPP)Co(R) in CH_2Cl_2 containing a substituted pyridine (L) are shifted negatively as compared to the half-wave potentials for oxidation of the same compound in neat CH_2Cl_2. The difference in $E_{1/2}$ between the five- and six-coordinate complexes ($\Delta E_{1/2}$) is related to the formation constant as well as to the ligand concentration in solution, [L]. This is shown in eq 4, where K_{red} and K_{ox} are the formation constants of (TPP)Co(R)(L) and $[(TPP)Co(R)(L)]^+$ (eqs 5 and 6, respectively).[31]

$$\Delta E_{1/2} = (2.3RT/F)\log\{(1 + K_{ox}[L])/(1 + K_{red}[L])\} \quad (4)$$

$$(TPP)Co(R) + L \overset{K_{red}}{\rightleftharpoons} (TPP)Co(R)(L) \quad (5)$$

$$[(TPP)Co(R)]^+ + L \overset{K_{ox}}{\rightleftharpoons} [(TPP)Co(R)(L)]^+ \quad (6)$$

The $E_{1/2}$ values for oxidation of (TPP)Co(R) (R = Et, Me, and Ph) in CH_2Cl_2 and CH_2Cl_2 containing L (1.0 × 10^{-2} M) are summarized in Table 4. The $E_{1/2}$ values of (TPP)Co(Ph) in the presence of L (1.0 × 10^{-2} M) were also determined in MeCN/$CHCl_3$ (4:1 v/v) and are listed in parentheses in Table 4.

Effects of Base on Migration Rate. Migration rates of $[(TPP)Co(R)(L)]^+$ (R = Ph and Me) were determined at 298 K by monitoring the increase in absorbance at λ_{max} due to [(*N*-RTPP)Co(L)]$^+$ in MeCN containing L (2.0 × 10^{-2} M). The migration rate constants (k_{mig}) are listed in Table 5 along with pK_a values of the substituted pyridines. As shown in Figure 7a, the k_{mig} values of $[(TPP)Co(Ph)(L)]^+$ *increase* by 1−2 orders of magnitude with increase in the ligand pK_a.

In contrast to the above linear relationship, the variations in logk_{mig} values of $[(TPP)Co(Me)(L)]^+$ with ligand pK_a show a nonlinear relationship, i.e., logk_{mig} first increases slightly, reaches a maximum for 3-chloropyridine (no. 3 in Table 5), and then *decreases* for all substituted pyridines with pK_a values larger than that of 3-chloropyridine (see Figure 8a).

Correlations of $E_{1/2}$ with the pK_a of the axial ligand are shown in Figures 7b and 8b for the oxidation of (TPP)Co(Ph)(L) and (TPP)Co(Me)(L), respectively. In each case, the $E_{1/2}$ values become more negative with increase in pK_a of the substituted pyridine. Thus, the axial ligand coordination on cobalt results in an increased electron density on the metal center from which an electron is removed. The formation constants (log*K*) of (TPP)Co(R)(L) (R = Ph and Me) also correlate with the pK_a of the axial ligand, and these relationships are shown in Figures 7c and 8c. Both log*K* values increase linearly with increase in the ligand pK_a.

Table 5. Rate Constants (logk_{mig}) for the Metal to Nitrogen R Group Migration of $[(TPP)Co(R)]^+$ and $[(TPP)Co(R)(L)]^+$ at 298 K in MeCN Containing 2.0 × 10^{-2} M Substituted Pyridine

sixth axial ligand, L			σ-bonded ligand, R logk_{mig}	
no.	type	pK_a[a]	Me	Ph
	none		−1.6	−2.9
1	3,5-Cl_2Py	0.67	−1.8	−2.7
2	4-CNPy	1.86	−1.6	−3.0
3	3-ClPy	2.81	−1.5	−2.8
4	Py	5.28	−2.0	−2.3
5	3-MePh	5.79	−1.6	
6	3,4-Me_2Py	6.46	−2.5	−1.5
7	4-NMe_2Py	9.71	*b*	*b*

[a] Taken from ref 30. [b] The oxidation of (TPP)Co(R)(L) by $[Fe(phen)_3]^{3+}$ does not occur in the presence of 4-NMe_2Py (no. 7) which may be due to an oxidation of the substituted pyridine instead of (TPP)Co(R)(L).

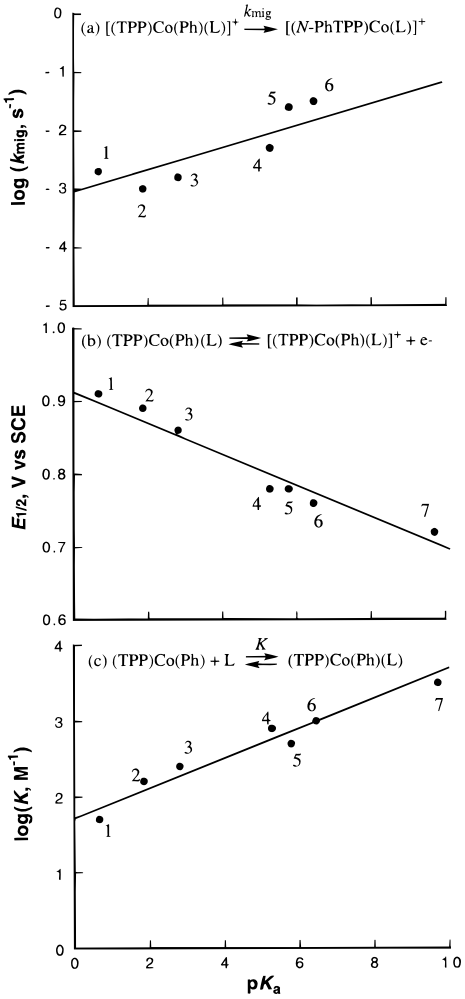

Figure 7. Correlation between the pK_a of the substituted pyridine and (a) the migration rate constant of $[(TPP)Co(Ph)(L)]^+$ in MeCN at 298 K, (b) the oxidation potential of (TPP)Co(Ph)(L) in CH_2Cl_2, and (c) the formation constant of (TPP)Co(Ph) in MeCN.

Effects of Base on ESR Spectra of Singly Oxidized Complex. The ESR spectra of $[(TPP)Co(Ph)]^+$ and [(TPP)-Co(Me)]$^+$ are identical in CH_2Cl_2 and have the same *g* (2.008) and A_{Co} (5.0 G) values (Table 6). The *g* and A_{Co} values are

(30) Shoefield, K. S. *Hetero-Aromatic Nitrogen Compounds*; Plenum Press: New York, 1967; p 146.

(31) For similar analysis, see: (a) Fukuzumi, S.; Kondo, Y.; Tanaka, T. *J. Chem. Soc., Chem. Commun.* **1985**, 1053. (b) Fukuzumi, S.; Kondo, Y.; Mochizuki, S.; Tanaka, T. *J. Chem. Soc., Perkin Trans. 2* **1989**, 1753.

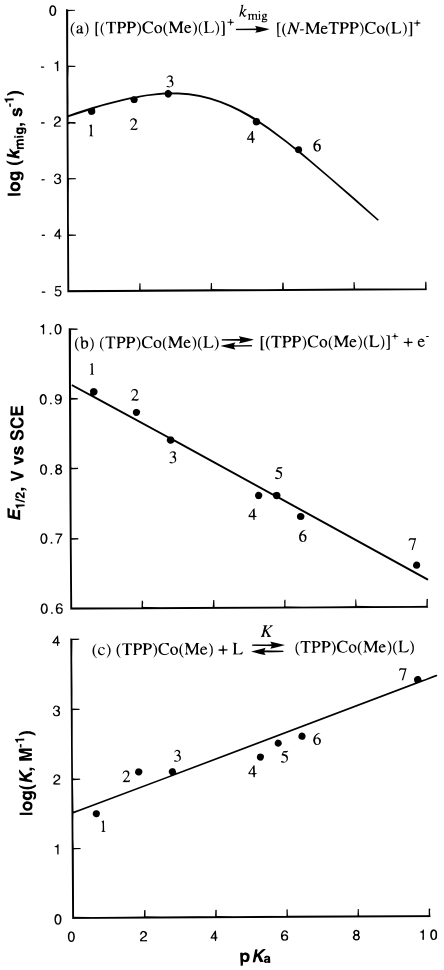

Figure 8. Correlation between the pK_a of the substituted pyridine and (a) the migration rate constant of $[(TPP)Co(Me)(L)]^+$ in MeCN at 298 K, (b) the oxidation potential of (TPP)Co(Me)(L) in CH_2Cl_2, and (c) the formation constant of (TPP)Co(Me) in MeCN.

Table 6. Isotropic g and A_{Co} Values of $[(TPP)Co(R)]^+$ in CH_2Cl_2 and (TPP)Co(R)(L in MeCN/$CHCl_3$ (1:1 v/v) Containing 0.40 M Ligands at 298 K[a]

sixth axial ligand, L			R = Ph		R = Me	
no.	type	pK_a	g	A_{Co}, G	g	A_{Co}, G
	none[b]		2.008	5.0	2.008	5.0
	MeCN		2.015	5.3	2.027	7.0
1	3,5-Cl_2Py	0.67	2.016	7.9	2.020	9.0
2	4-CNPy	1.86	2.016	8.2	2.021	9.9
3	3-ClPy	2.81	2.016	8.4	2.021	11.5
4	Py	5.28	2.017	8.6	2.023	12.6
5	3-MePy	5.79	2.023	12.1	2.023	12.6
6	3,4-Me_2Py	6.46	2.023	12.1	2.023	12.6
7	4-NMe_2Py	9.71	2.025	11.7	2.020	12.2

[a] Cationic species was produced in an ESR cell by oxidation with $[Fe(phen)_3](ClO_4)_3$ and measurements made immediately afterward. [b] Measured in CH_2Cl_2.

similar to those of the $[(TPP)Co^{III}]^{2+}$ porphyrin π radical cation (g = 2.003, A_{Co} = 6.0 G),[21] suggesting that both $[(TPP)Co(Ph)]^+$ and $[(TPP)Co(Me)]^+$ in a noncoordinating solvent such as CH_2Cl_2 can be best described as a cobalt(III) π radical cation. On the other hand, when the ESR spectra of $[(TPP)Co(Ph)]^+$ and $[(TPP)Co(Me)]^+$ are measured in MeCN/$CHCl_3$, the isotropic g (2.027 ± 0.001) and A_{Co} (7.0 G) values of $[(TPP)Co(Me)(MeCN)]^+$ are different from those of $[(TPP)Co(Ph)(MeCN)]^+$ (g = 2.015 and A_{Co} = 5.3 G), reflecting more Co(IV) character in the singly oxidized σ-bonded methyl derivative

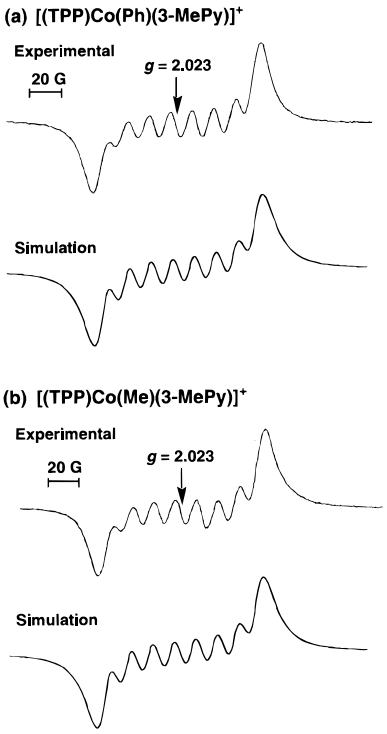

Figure 9. Experimental ESR spectra and computer simulation spectra of (a) $[(TPP)Co(Ph)(3\text{-}MePy)]^+$ (5.0 mM) and (b) $[(TPP)Co(Me)(3\text{-}MePy)]^+$ (5.0 mM) generated by addition of 5.0 mM $[Fe(phen)]_3^{3+}$ to (TPP)Co(Ph) and (TPP)Co(Me) in MeCN/$CHCl_3$ (v:v 1/1) containing 0.40 M 3-MePy at 208 K.

containing a bound MeCN molecule, $[(TPP)Co(Me)(MeCN)]^+$ than in $[(TPP)Co(Ph)(MeCN)]^+$ (see Table 6). However, when a strong base (L) is added to the MeCN/$CHCl_3$ solution, the resulting $[(TPP)Co(Ph)(L)]^+$ and $[(TPP)Co(Me)(L)]^+$ species again have almost identical ESR spectra. The striking similarity in the ESR spectra of $[(TPP)Co(Ph)(L)]^+$ and $[(TPP)Co(Me)(L)]^+$ is shown in Figure 9 for the case of L = 3-MePy. Figure 9 also illustrates the computer-simulated spectra of the two complexes.

The ESR parameters of $[(TPP)Co(Ph)(L)]^+$ and $[(TPP)Co(Me)(L)]^+$ are summarized in Table 6. The g value of $[(TPP)Co(Ph)(L)]^+$ increases with increase in the ligand pK_a to reach a maximum value which is consistent with formation of a genuine Co(IV) complex.[7] In the case of the Me derivative, the coordination of MeCN is strong enough to change the oxidation state from Co(III) for $[(TPP)Co(Me)]^+$ in CH_2Cl_2 to Co(IV) for $[(TPP)Co(Me)(MeCN)]^+$ in MeCN/$CHCl_3$. In addition, the coordination of a base (L) which is stronger than MeCN results in no further significant changes in either the g or A_{Co} values of $[(TPP)Co(R)(L)]^+$ (R = Ph and Me). The fact that the g and A_{Co} values do not vary upon changing the pK_a of the ligand also confirms that $[(TPP)Co(R)(L)]^+$ can best be described as a d^5 cobalt(IV) complex.

Site of Electron Transfer Prior to Migration. The above results can be explained by the reactions shown in Scheme 3 for (TPP)Co(Me) and (TPP)Co(Ph) prior to the migration step. A transient $[(TPP)Co^{III}(R)]^+$ species is invariably formed upon oxidation in CH_2Cl_2 but this is not the case in MeCN where either $[(TPP)Co^{III}(R)(MeCN)]^+$ or $[(TPP)Co^{IV}(R)(MeCN)]^+$ are formed depending on the specific σ-bonded axial ligand.

The higher the oxidation state of the singly oxidized compound, i.e., the more its Co(IV) character, the faster the migration rate. This result is best seen in the case of the Ph derivative where the Co(IV) character first increases upon going

Scheme 3

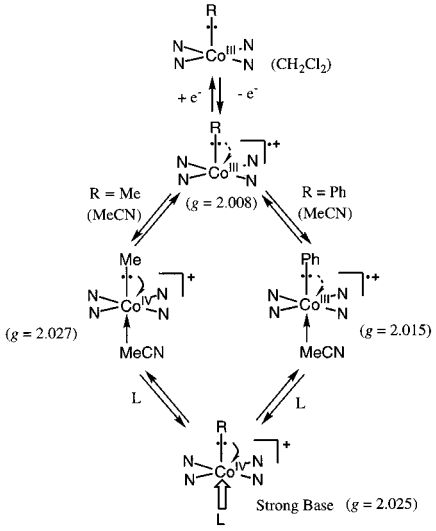

from $[(TPP)Co(Ph)]^+$ to $[(TPP)Co(Ph)(L)]^+$ and then further increases with increase in the ligand pK_a, thus resulting in an acceleration of the migration rate. In contrast, $[(TPP)Co(Me)(MeCN)]^+$ already contains a Co(IV) metal center and a conversion of $[(TPP)Co^{IV}(Me)(MeCN)]^+$ to $[(TPP)Co^{IV}(Me)(L)]^+$ by axial ligand coordination thus increases the electron density on the cobalt, resulting in a slower migration rate. Thus, the cleavage of the cobalt−carbon bond in the migration reaction occurs via a rate-determining intramolecular electron transfer from R to Co, which results in a metal to nitrogen migration of the R group.

Comparison of Bond Energies for Co(III)− and Co(IV)−Carbon Bonds. Cobalt−carbon bond dissociation energies of organocobalt(III) complexes have previously been determined using the kinetic analysis of homolytic cleavage of cobalt−carbon bond.[32,33] The cobalt−carbon bond dissociation energies of (TPP)Co(R) can be determined in a similar fashion and compared with the bond energies for the singly oxidized $[(TPP)Co(R)]^+$ complexes. The rates of homolytic cleavage of the cobalt−carbon bond in (TPP)Co(R) were determined by monitoring both the decrease of the 406 nm band and the increase of bands due to (TPP)Co formation in MeCN containing a TEMPO radical trap.[32−34] The rates obey first-order kinetics with respect to the (TPP)Co(R) concentration (eq 7). The observed first-order rate constants increase with the TEMPO concentration and approach a constant value as shown in Figure 10 for the case of (TPP)Co(Bu). Such a saturated dependence

$$-\frac{\mathrm{d}[(TPP)Co(R)]}{\mathrm{d}t} = k_{obs}[(TPP)Co(R)] \qquad (7)$$

of the rate constant on the TEMPO concentration indicates that radicals generated by the homolytic cleavage of the cobalt−carbon bond are trapped by the TEMPO radical before they recombine with the Co(II) center (see Scheme 4). According

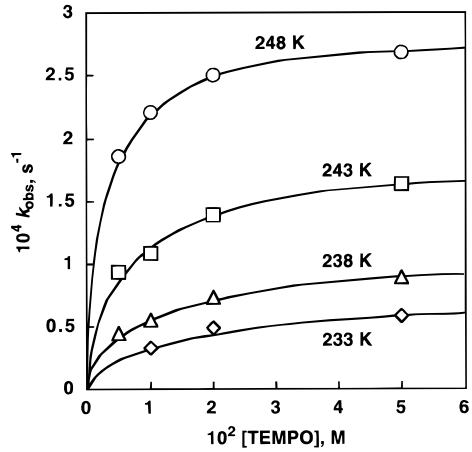

Figure 10. Plot of k_{obs} vs [TEMPO] for the anaerobic thermolysis of (TPP)Co(Bu) (5.0×10^{-6} M) in MeCN at various temperatures.

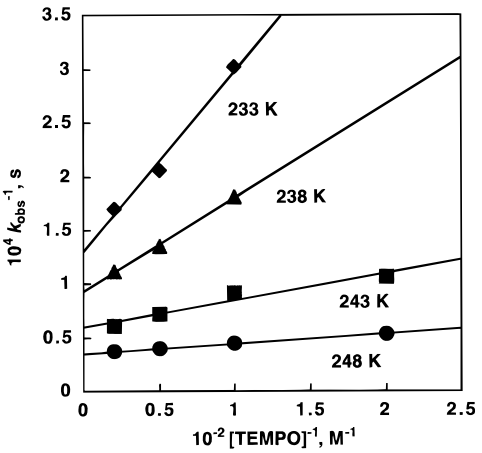

Figure 11. Plot of k_{obs}^{-1} vs $[TEMPO]^{-1}$ for the anaerobic thermolysis of (TPP)Co(Bu) (5.0×10^{-6} M) in MeCN at various temperatures.

Scheme 4

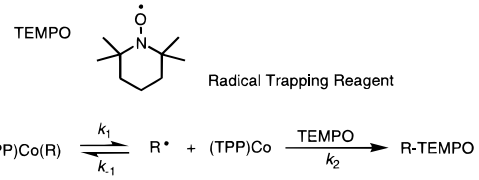

to this scheme, eq 8 can be derived and will show a linear correlation between k_{obs}^{-1} and $[TEMPO]^{-1}$. Such linear plots can be experimentally observed as shown in Figure 11.[35]

$$\frac{1}{k_{obs}} = \frac{1}{k_1} + \frac{k_{-1}[(TPP)Co]}{k_1 k_2[TEMPO]} \qquad (8)$$

The k_1 values for homolytic cleavage of the cobalt−carbon bond in (TPP)Co(R) are obtained from the intercepts. The activation parameters ($\Delta H^{\ddagger}$ and $\Delta S^{\ddagger}$) are obtained from Eyring plots and these values are listed in Table 7. The activation enthalpies ($\Delta H^{\ddagger}$) and entropies ($\Delta S^{\ddagger}$) for the R group migration of $[(TPP)Co(R)]^+$ are obtained from the Eyring plots of k_{mig}, and these values are also listed in Table 7. The $\Delta S^{\ddagger}$ values of (TPP)Co(R) and $[(TPP)Co(R)(MeCN)]^+$ do not vary significantly with the different R groups (see Table 7), and the difference in reactivity between the neutral and oxidized complexes is

(32) (a) Halpern, J. *Acc. Chem. Res.* **1982**, *15*, 238. (b) Halpern, J. *Pure Appl. Chem.* **1983**, *55*, 1059.

(33) (a) Tsou, T.-T.; Loots, M.; Halpern, J. *J. Am. Chem. Soc.* **1982**, *104*, 623. (b) Ng, F. T. T.; Rempel, G. L.; Halpern, J. *J. Am. Chem. Soc.* **1982**, *104*, 621. (c) Geno, M. K.; Halpern, J. *J. Am. Chem. Soc.* **1987**, *109*, 1238. (d) Finke, R. G.; Smith, B. L.; Mayer, B. J.; Molinero, A. A. *Inorg. Chem.* **1983**, *22*, 3677. (e) Riordan, C. G.; Halpern, J. *Inorg. Chim. Acta* **1996**, *243*, 19.

(34) Koenig, T.; Finke, R. G. *J. Am. Chem. Soc.* **1988**, *110*, 2657; Garr, C. D.; Finke, R. G. *J. Am. Chem. Soc.* **1992**, *114*, 10440; Garr, C. D.; Finke, R. G. *Inorg. Chem.* **1993**, *32*, 4414.

(35) The [Co(II)]/[TEMPO] dependence in eq 7 has been well established. See refs 32−34.

Table 7. Activation Enthalpies ($\Delta H^{\ddagger}$) and Entropies ($\Delta S^{\ddagger}$) for Homolytic Cleavage of the Co−R Bond of (TPP)Co(R) and for R Group Migration of $[(TPP)Co(R)]^+$

	$\Delta H^{\ddagger}$, kcal mol^{-1} [a]		$\Delta S^{\ddagger}$, cal K^{-1} mol^{-1} [a]	
R	(TPP)Co(R)	$[(TPP)Co(R)]^+$	(TPP)Co(R)	$[(TPP)Co(R)]^+$
Bu	19.3	8.4	−19.7	−16.3
Et	19.8	8.7	−19.1	−18.1
Me	19.7	14.5	−20.0	−18.8
Ph		15.0		−21.7

[a] The experimental error is ±5%.

therefore ascribed to differences in the $\Delta H^{\ddagger}$ values. It is important to note that the $\Delta S^{\ddagger}$ value for homolytic cleavage of the cobalt−carbon bond in $(TPP)Co^{III}(Me)$ (−20.0 cal K^{-1} mol^{-1}) agrees well with the $\Delta S^{\ddagger}$ value for the R group migration of $[(TPP)Co^{IV}(Me)]^+$ (−18.8 cal K^{-1} mol^{-1}). Such an agreement between the two values also supports the migration mechanism shown in Scheme 2, where the homolytic cleavage of the Co−R bond in $[(TPP)Co^{IV}(R)]^+$ is the rate-determining step for the R migration.

The $\Delta H^{\ddagger}$ values can be converted to the Co(III)−R dissociation energy (D_{Co-R}) by using eq 9, where F_c is the ratio of cage recombination to the sum of all competing cage processes and

$$D_{Co-R} = \Delta H^{\ddagger} - F_c \Delta H^{\ddagger}_{\eta} \qquad (9)$$

$\Delta H^{\ddagger}_{\eta}$ is the activation enthalpy for viscous flow.[34,36] Since $0 < F_c < 1$ and $1 < \Delta H^{\ddagger}_{\eta} < 2$ kcal mol^{-1}, the $F_c \Delta H^{\ddagger}_{\eta}$ value may be taken as 1 ± 1 kcal mol^{-1}. The D_{Co-R} values for (TPP)-Co(R) are similar to those for other organocobalt(III) complexes with the same σ-bonded organic groups[31,32] but are significantly larger than those for the corresponding Co(IV) complexes. Thus, the cobalt−carbon bond in the high oxidation state Co(IV) complex becomes significantly weaker as compared to that in the lower oxidation state Co(III) complex.[37]

Acknowledgment. This work was partially supported by an International Scientific Research Program (No. 08044083) from the Ministry of Education, Science, Culture and Sports, Japan. K.M.K. also acknowledges support from the Robert A Welch Foundation (Grant E−680).

Supporting Information Available: Derivation of eq 1, a typical kinetic figure, tables of spectral data for neutral and oxidized (TPP)Co(R) and R-migrated products, figures of the spectral changes observed in the absence and presence of various substituted pyridines, table of formation constants, and a figure of spectral changes for the complexation of (TPP)Co(R) with substituted pyridines (9 pages). See any current masthead page for ordering and Web access instructions.

JA973257E

(36) Koenig, T. W.; Hay, B. P.; Finke, R. G. *Polyhedron* **1988**, 7, 1499.

(37) The facile homolytic cleavage for the cobalt−carbon bonds of alkylcobalt(IV) complexes has been well-documented as compared to the slow cleavage of the corresponding alkylcobalt(III) complexes, which requires thermal or photochemical activation, see: Ishikawa, K.; Fukuzumi, S.; Goto, T.; Tanaka, T. *J. Am. Chem. Soc.* **1990**, *112*, 1577. Fukuzumi, S.; Ishikawa, K.; Tanaka, T. *Organometallics* **1987**, *6*, 358. Ishikawa, K.; Fukuzumi, S.; Tanaka, T. *Bull. Chem. Soc. Jpn.* **1987**, *60*, 563. Fukuzumi, S.; Kitano, T.; Ishikawa, M.; Matsuda, Y. *Chem. Phys.* **1993**, *176*, 337.